# Optical quasi-three-dimensional correlation

Youzhi Li[1], Joseph Rosen[2]
Department of Electrical and Computer Engineering, Ben-Gurion University of the Negev
P. O. Box 653, Beer-Sheva, 84105, Israel

## ABSTRACT

A novel optical correlator for three-dimensional (3-D) object recognition is proposed herein. Several projections of a 3-D scene are recorded under white light illumination and fused into a single complex two-dimensional function. After properly filtering this function, it is then coded into a computer-generated hologram (CGH). When the CGH is coherently illuminated, a correlation space between the 3-D tested scene and the reference function is reconstructed, in which light peaks indicate on the existences and locations of true targets in the observed 3-D scene. Experimental results are presented.
**Keywords:** Three-dimensional optical correlation, Pattern recognition and feature extraction, Computer-generated hologram.

## 1. INTRODUCTION

Recently, there has been increasing interest in three-dimensional (3-D) optical information processing because of its potential applications. A method for performing 3-D optical correlation was first proposed by Bamler and Hofer-Alfeis[1], in which the 3-D observed scene is first mapped, slice by slice along its longitudinal axis, onto a large 2-D plane. Then, conventional 2-D optical correlations are performed between every slice with all the others. In this method the observed scene must be processed with intensive digital algorithms to reconstruct the 3-D image inside the computer memory before any correlation can be employed. Recently other attempts of 3-D optical pattern recognition were reported[2-9]. Rosen has proposed to extend the correlation dimensions from 2-D to 3-D by introducing 3-D optical Fourier transform (FT)[2,3]. By fusing several projections of the tested scene, a 3-D object function is first Fourier transformed, filtered by some 3-D reference filter and finally inversely Fourier transformed into the correlation space. By this technique a target can be detected and located in its 3-D environment. His method has been firstly demonstrated with a 3-D joint transform correlator (JTC)[4]. Later, we have proposed a method to implement 3-D distortion invariance for the 3-D pattern recognition by use of a single 2-D synthetic reference function in the 3-D JTC[5]. As an alternative to the 3-D JTC, we have also proposed a hybrid 3-D correlator with general complex filters[6]. Esteve-Taboada *et. al.* have suggested to combine the Fourier transform profilometry technique[10] with a conventional 2-D optical correlator for performing the 3-D object recognition[7]. Frauel *et. al.* have proposed a different 3-D object recognition technique using digital holography[8]. First, 2-D various viewpoint projections of the 3-D observed scene are reconstructed from a digital hologram. Then, the system recognizes the true targets included in the tested 3-D scene by use of 2-D correlation techniques. Matoba *et. al.* have captured multiple perspectives of 3-D objects by a microlens array[9]. The various perspectives of the reference and the input scene are cross-correlated by a 2-D JTC, whereas the depth information of the 3-D objects is converted to angular information of the perspectives.

The main criticism on all the various versions of the 3-D correlators developed at Ben-Gurion University[2-6] (BGU correlators, hereafter) has been directed against their complexity and their extensive use of digital computation. To overcome these drawbacks, we propose herein a new 3-D pattern recognition system, termed 3-D optical quasi-correlator (OQC). This system is a degenerate version of the hybrid BGU correlator[6]. It can still recognize and locate objects in 3-D space, and thus the 3-D space invariance property is maintained. However, the recognition in the 3-D OQC is not done by a complete 3-D correlation. Therefore, in a few aspects, like simplicity and operation speed, the new system is superior over the BGU correlators. However, there is some penalty for this simplicity by mean of reduction of the

[1] li@ee.bgu.ac.il; Tel: +972-8-6461841; http://www.ee.bgu.ac.il/~li;
[2] rosen@ee.bgu.ac.il; Tel: +972-8-6477150; http://www.ee.bgu.ac.il/~rosen;


Algorithms and Systems for Optical Information Processing VI, Bahram Javidi, Demetri Psaltis, Editors, Proceedings of SPIE Vol. 4789 (2002) © 2002 SPIE · 0277-786X/02/$15.00

system's performances. For instance, the signal to noise ratio is reduced compared to its value in the BGU correlators, as demonstrated in the last section.

The main difference between the 3-D OQC and the BGU correlators exists in their output stage. In the BGU correlators each transversal slice of the 3-D correlation space is reconstructed separately from a different computer generated hologram (CGH). In the 3-D OQC, on the other hand, only a single CGH is used to reconstruct the intensity distribution of the entire 3-D correlation space at once. Therefore, the detection method of the correlation peaks should be modified. The correlation peaks are not necessarily distributed on a single transverse plane, which can be recorded by a conventional planar detector. Instead, one needs an imaging system that is capable of observing the entire 3-D correlation space. Such system can be, for instance, the human vision system, which enables anyone with a stereoscopic vision to observe the correlation peaks and estimate their locations in the 3-D space. An artificial imaging system, which imitates this kind of human ability, is an additional option that should be considered in this context.

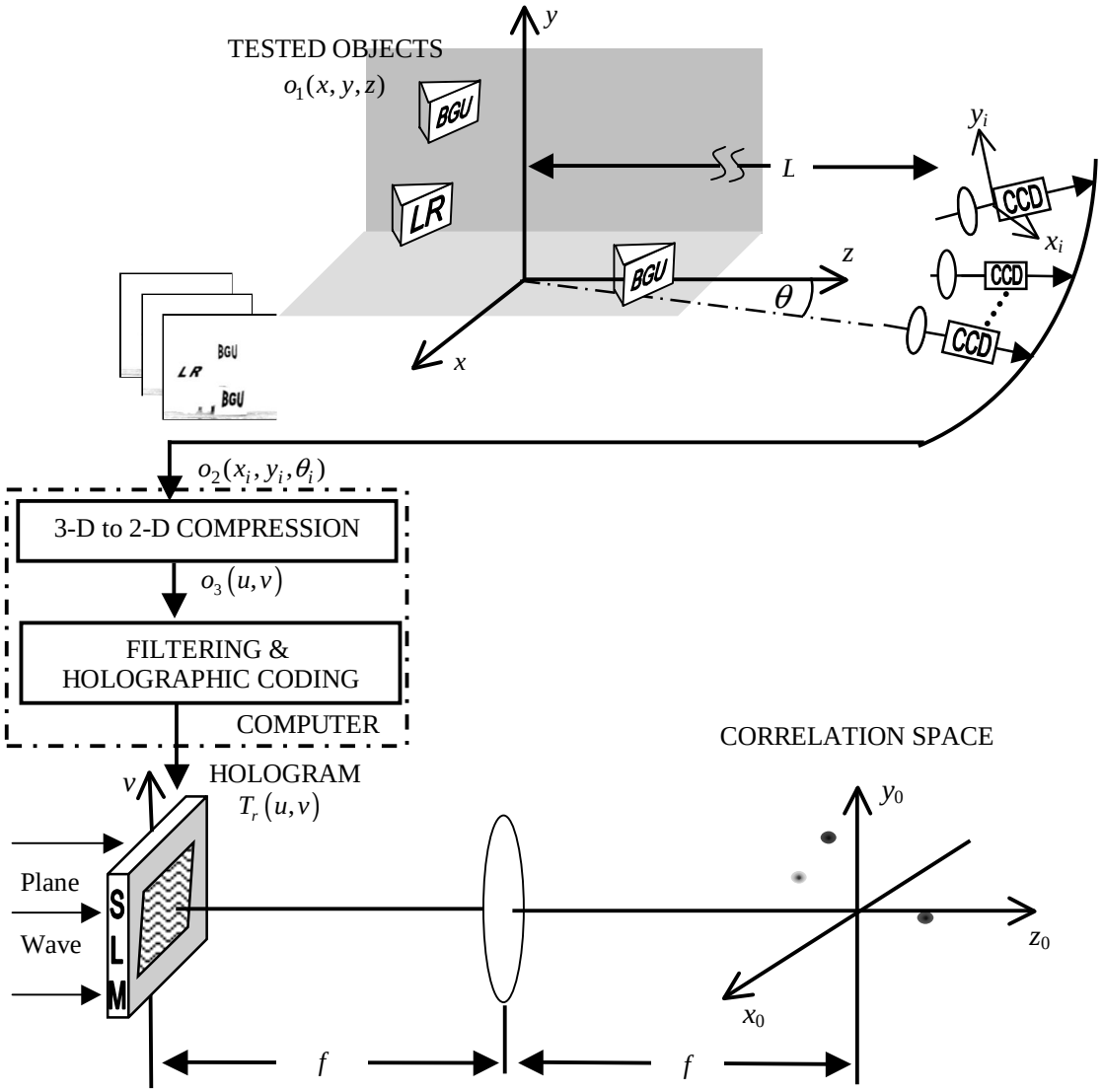


**Fig. 1** The schematic of the proposed system

## 2. SYSTEM'S ANALYSIS

The image capturing processes by the 3-D OQC and by the BGU correlators are identical, and such process was already described in Ref. 6. Nevertheless, for the completeness, we repeat the description of this part in the following.

The complete proposed scheme is shown in Fig. 1. The input function containing several objects is denoted by $o_1(x,y,z)$, where $(x,y,z)$ are the coordinates of the observed scene. A digital camera, located a distance L from the origin, captures the objects $o_1(x,y,z)$ from several different points of view. The digital camera is shifted in constant angular steps along a horizontal arc centered on the origin, where the camera is always directed to the origin. The angle between the optical axis of the digital camera and the $z$ axis is denoted by $\theta_i$. For each $\theta_i$, the projected image $o_2(x_i, y_i, \theta_i)$ is recorded into the computer, where ($x_i$, $y_i$) are the coordinates of the image plane of each camera. Based on simple geometrical considerations, the relation between $(x_i, y_i)$ and $(x, y, z, \theta_i)$ is given by

$$(x_i, y_i) = M(x\cos\theta_i + z\sin\theta_i, y) \qquad (1)$$

where $M$ is the magnification factor of the digital camera. Assuming the distance L is much longer than the depth of the 3-D input scene, all the object points of the 3-D input scene are equally imaged with the same magnification factor $M$.

Inside the computer, the processing is different from that of the BGU correlators. In the BGU correlators the computation process of the angular projections has yielded 3-D FT of the scene. Then, after appropriate filtering and another 3-D FT, we have obtained 3-D correlation between a reference and the scene objects. Here the output stage of the OQC is different than that of the BGU correlators, and therefore the computational processing is changed. In the OQC output, a Fourier hologram is coherently illuminated, and as a result, the 3-D correlation space is reconstructed in front of the observer eyes. The desired hologram has only two dimensions, even it represents 3-D scene, and therefore the 3-D data of the angular projections should be compressed properly into a two-dimensional function. This compression is the goal of the computational process as described next.

The set of captured images are compressed in a special way to a single spectral matrix. The digital operations along the horizontal and the vertical axes are different because the camera collects the angular projections only along the horizontal axis. As the analysis shows in the following, the entire spatial spectrum information of every projection along the $x_i$-axis is redundant. For each $k$-th projection from the view angle $\theta_k$ we just calculate, and store, the spectral content of the $u_k$-th frequency element, where $u_k$ and $\theta_k$ are related by the relation $u_k=\theta_k/a$, and $a$ is some chosen parameter. In other words, from the spatial spectrum of each projected image a different column is picked up according to the above-mentioned rule. Of course, there is no need to calculate the complete horizontal spectrum of every projection, but only the columns from the spectrum, that are used in the new obtained matrix. Each $k$-th projection is multiplied by $\exp(-j2\pi x_i u_k/\lambda f)$, and the product is summed up along the rows (i.e. along $x_i$) to a single column. $\lambda$ is the wavelength of a plane wave illuminating the output hologram, and $f$ is the focal length of the spherical Fourier lens used later in the system's output. As we show later, the parameter $a$ controls the longitudinal magnification of the correlation space independently of the transverse magnification. In this stage, the entire projected matrices are compressed together to a single 2-D matrix, which is then Fourier transformed along $y_i$-axis, with a scale factor of $1/(\lambda f)$. Thus, in continuous formalism, the dimension of the grabbed data is reduced from three to two in the following way,

$$o_3(u,v) \propto \iint o_2(x_i, y_i, au)\exp\left[-j2\pi\left(ux_i + vy_i\right)/\lambda f\right]dx_i dy_i \qquad (2)$$

Note that there is no Fourier transform along $x_i$ because for each frequency value $u$ the integration is done on a different projection according to the relation $\theta_i = au$. It should be noted that although the rule of compressing seems arbitrary, the relation $\theta_i = au$ leads to the desired Fourier hologram as shown in the following.

The maximum view angle $\theta$ is chosen to be small (in the current example, it is $16^0$ from each side of $z$-axis), thus we can employ the small angle approximation: $\cos\theta_i \approx 1$ and $\sin\theta_i \approx \theta_i$. Substituting Eq. (1), the small-angle approximations and the relation $\theta_i = au$ into relation (2) yields

$$o_3(u,v) \propto \iint o_2(x_i, y_i, au) \exp\left[-j2\pi M \left(ux + vy + au^2 z\right) \Big/ \lambda f\right] dx_i dy_i \qquad (3)$$

Let us look on a single element from the entire 3-D object function. This infinitesimal element of the size ( $\Delta x, \Delta y, \Delta z$ ), at point $(x, y, z)$, and with brightness $o_1(x, y, z)$, appears as a single element on every projection plane, but at a different location from projection to projection according to Eq. (1). Therefore, in this case the spectrum presented in relation (3) is given by

$$o_3(u,v) \propto o_1(x, y, z) \exp\left[-j2\pi M \left(ux + vy + au^2 z\right) \Big/ \lambda f\right] \Delta x \Delta y \Delta z \qquad (4)$$

Next we examine the influence of all points of the tested scene $o_1(x, y, z)$ on the distribution of $o_3(u,v)$. The tested scene is three-dimensional, and therefore, the overall distribution of $o_3(u,v)$ is obtained as a 3-D integral of all the points from the input scene, as follows,

$$o_3(u,v) \propto \iiint o_1(x, y, z) \exp\left[-j2\pi M \left(ux + vy + au^2 z\right) \Big/ \lambda f\right] dx dy dz \qquad (5)$$

Thus we obtain a 2-D function, which contains 3-D information of the tested scene in a similar sense that a 2-D optical hologram contains the 3-D information of the recorded 3-D scene[11]. $o_3(u,v)$ is first multiplied by a proper filter, and then the obtained product is encoded into a CGH. The CGH, when illuminated by a plane wave, yields a holographic reconstruction of the correlation space, as shown in the lower part of Fig. 1. Thus, we can detect the targets, and also locate them in their 3-D environment.

To implement the 3-D object recognition we next consider the filter function defined by

$$F(u,v) \propto \iiint f^*(-x, -y, -z) \exp\left[-j2\pi M \left(ux + vy + au^2 z\right) \Big/ \lambda f\right] dx dy dz \qquad (6)$$

where $f(x,y,z)$ is the spatial reference function located at the origin of the coordinate system $(x,y,z)$, and the asterisk denotes complex conjugate. Multiplying $o_3(u,v)$ given by relation (5) with the filter function given by relation (6) yields

$$\begin{aligned} T(u,v) = o_3(u,v)F(u,v) &\propto \iiint o_1(x, y, z) \exp[-j2\pi M (ux + vy + au^2 z) / \lambda f] dx dy dz \\ &\quad \times \iiint f^*(-\xi, -\eta, -\zeta) \exp[-j2\pi M (u\xi + v\eta + au^2 \zeta) / \lambda f] d\xi d\eta d\zeta \\ &= \iiint \iiint o_1(x, y, z) f^*(-\xi, -\eta, -\zeta) \\ &\quad \times \exp\{-j2\pi M [u(x + \xi) + v(y + \eta) + au^2 (z + \zeta) / \lambda f\} dx dy dz \quad d\xi d\eta d\zeta \\ &= \iiint \iiint o_1(x, y, z) f^*(x - \hat{x}, y - \hat{y}, z - \hat{z}) dx dy dz \\ &\quad \times \exp[-j2\pi M (u\hat{x} + v\hat{y} + au^2 \hat{z}) / \lambda f] d\hat{x} d\hat{y} d\hat{z} \\ &= \iiint g(\hat{x}, \hat{y}, \hat{z}) \exp[-j2\pi M (u\hat{x} + v\hat{y} + au^2 \hat{z}) / \lambda f] d\hat{x} d\hat{y} d\hat{z} \qquad (7) \end{aligned}$$

where

$$g(\hat{x}, \hat{y}, \hat{z}) = \iiint o_1(x, y, z) f^*(x - \hat{x}, y - \hat{y}, z - \hat{z}) dx dy dz \qquad (8)$$

$$\hat{x} = x + \xi$$

and $\hat{y} = y + \eta$

$$\hat{z} = z + \zeta$$

The function $g(\hat{x}, \hat{y}, \hat{z})$ is the 3-D correlation between the tested object function and the reference function. The 2-D function $T(u, v)$ is generally complex-valued and in this stage it is stored inside the computer memory.

Looking over the last line of relation (7) we note that there is not symmetry between the horizontal coordinate $u$ and the vertical coordinate $v$. In the argument of the exponent one finds the term $au^2z$ without the term $av^2z$. This is because the recording process is not symmetric since all the recorded projections are horizontal-only viewpoints. If we could collect all the projections along the horizontal as well as the vertical viewpoints, relation (7) would become symmetrical. In such hypothetical case the function $T(u, v)$ could become

$$\tilde{T}(u,v) = \iiint g(\hat{x}, \hat{y}, \hat{z}) \exp\{-j2\pi M [u\hat{x} + v\hat{y} + a(u^2 + v^2)\hat{z}] / \lambda f\} d\hat{x} d\hat{y} d\hat{z} \qquad (9)$$

In order to understand the way that the correlation function $g(\hat{x},\hat{y},\hat{z})$ can be obtained from $\tilde{T}(u,v)$, we have to look for equivalent optical system that yields the same distribution of $\tilde{T}(u,v)$. Such system is well known in the literature for the parameter value *a=-1/2f*. When $g(\hat{x},\hat{y},\hat{z})$ is located in the vicinity of the front focal point of a spherical lens, and illuminated by a plane wave, the 2-D complex amplitude on the back focal plane of this lens is equal to $\tilde{T}(u,v)$ given by Eq. (9)[12] for *a=-1/2f*. Therefore, based on the principle of optical reciprocity, if $\tilde{T}(u,v)$ located at the front focal plane, is encoded as a hologram and this hologram is illuminated by a plane wave, the 3-D distribution $g(\hat{x},\hat{y},\hat{z})$ is reconstructed in the vicinity of the back focal point of the lens. $g(\hat{x},\hat{y},\hat{z})$, as mentioned above, is the 3-D spatial distribution of the cross-correlation between the object function $o_1(\hat{x},\hat{y},\hat{z})$ and the reference function $f(\hat{x},\hat{y},\hat{z})$. Note that choosing a different value for the parameter *a* changes only the proportions between the transverse and the longitudinal dimensions of the reconstructed space, as already discussed in Ref. 11.

Unfortunately because of the scanning direction along the horizontal axis only, the distribution we can encode into a hologram is $T(u,v)$ but not $\tilde{T}(u,v)$. As a result the system inherently suffers from astigmatism, where the correlation peaks are focused along the *x* axis in different locations than they are focused along the *y* axis. Because of the term of $au^2z$ the correlation peaks are focused along the horizontal axis in the locations of the true objects at the input space, while because of missing of the term of $av^2z$ the same correlation peaks are focused along the vertical axis on the back focal plane of the reconstructing lens. This means that if a true object is located somewhere out of the origin, its correlation peak appears out of the back focal plane as a small line along the vertical axis instead of a point. Identifying the location of an object along the longitudinal axis should be done according to the measure of focusing along the horizontal axis only.

The astigmatism described above is one reason for the lower SNR in comparison to the result of the BGU correlators. As mentioned above the astigmatism is avoidable if the scanning of the input scene is performed along all the directions of a transversal plane. Therefore the astigmatism can be considered as a preventable problem that can be removed with an improved technology. However there is unavoidable source of noise, which is inherent to the holographic reconstruction. When there are several true objects, distributed in the scene in different transverse planes, the beam, which creates a correlation peak for each true object passes through all the rest of transverse planes and induces noise on all of them. This phenomenon distinguishes the obtained QOC holographic reconstruction from the real 3-D cross-correlation distribution obtained by the BGU correlators, and this is the reason that this system is considered as a quasi-correlator only.

As mentioned above, the hologram values are memorized inside the computer in a form of the complex function $T(u, v)$. To reconstruct the correlation space from the complex function, the computer should modulate some transparency medium with $T(u,v)$ values. In case the transparency cannot be modulated directly with complex values, one of many well-known coding methods of CGH's[13] might be used. The spatial light modulator (SLM) we use in this study can modulate an incident wave with positive gray-tones. Therefore, the complex function $T(u, v)$ is coded into a positive real transparency as follows

$$T_r(u,v) = 0.5\left(1+\mathrm{Re}\left\{T(u,v)\exp\left[\frac{i2\pi}{\lambda f}\left(d_x u + d_y v\right)\right]\right\}\right), \qquad (10)$$

where $(d_x, d_y)$ is the new origin point of the reconstruction space, and $|T(u,v)|$ is normalized between 0 and 1.

The holographic reconstruction setup is shown in the lower part of Fig. 1. The SLM modulated by $T_r(u,v)$ is illuminated by a plane wave, which propagates through the Fourier lens toward the observer. $T_r(u,v)$ given in Eq. (10) contains, among others, the term $T^*(u, v)$. From a Fourier transform of this term one can get the output correlation peaks with the same orientation as the original objects in the vicinity of the point $(x_0, y_0, z_0) = (-d_x, -d_y, 0)$, where $z_0 = 0$ designates the back focal plane of the Fourier lens.

## 3. EXPERIMENTAL RESULTS

To test our proposed scheme, an experiment was carried out, as described next. In this preliminary experiment, the tested 3-D scene included three objects with labels on their front faces, shown in the upper part of the Fig. 1. Two of them with the letters 'BGU' on their faces were the true targets that should be detected by the proposed system. The lower front object was located at the point $(x,y,z)=(0,0,5.6)$cm, whereas the higher back object was put at the point (-3,12.5,-5.4)cm (both with the letters 'BGU'). The object with the letters 'LR' located at the point (3,8.5,-5.4)cm, was used as the false target. This object should be ignored by the system. One digital camera observed the scene from a distance $L$=120cm from the origin of the tested scene. The camera was shifted along an arc centered at the origin. At each position, the camera was always directed toward the origin, and captured each projected image into a computer. The total view angle interval was $32^0$, $16^0$ for each side of the $z$-axis. The camera was shifted by $0.5^0$ from point to point. Thus, sixty-five projections of the 3-D tested scene were recorded into the computer, sixteen of them are depicted in Fig. 2 with a gap of $2^0$ between every two consecutive projections. The spectral matrix $o_3(u,v)$ generated from these data is shown in Fig. 3, where Fig. 3(a) and 3(b) are its amplitude and phase angle, respectively.


**Fig. 2** 16, out of 65 projections of the tested scene, imaged from $-16^0$ to $16^0$.

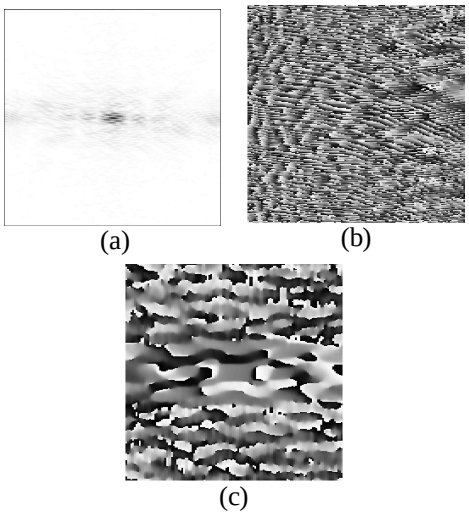


**Fig. 3** The amplitude (a) and the phase function (b) of the compressed spatial spectrum of the scene. (c) The phase function of the 3-D POF

The reference object was located at the origin of the scene, and imaged into the computer in the same method as described above, i.e. the observed reference object was recorded 65 times from different viewpoints by the CCD into the computer. From the recorded projections of the reference object we calculated a phase-only filter (POF), first by calculating the spectral matrix according to Eq. (2), and then by taking only the phase distribution of this matrix. The phase distribution of the POF function $F(u,v)$ is shown in Fig. 3(c). The multiplication result $T(u,v)$, of $o_3(u,v)$ with $F(u,v)$, was then encoded as a CGH $T_r(u,v)$ according to Eq. (10). The central part of the obtained hologram is shown in Fig. 4. To reconstruct the correlation space, both simulation and optical experiment were carried out. Fig. 5 shows the correlation results of the simulation, whereas the peaks in Figs. 5(a) and 5(b) indicate

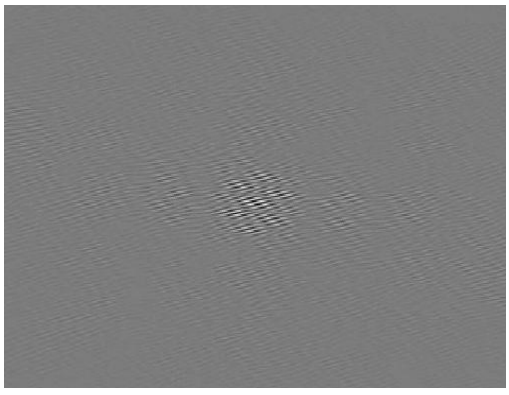

**Fig. 4** The central part of the CGH generated from T(u,v) by use of holographic coding

the existences and locations of the front and the back true targets. Figs. 5(c) and 5(d) are the 3-D plots of the intensity distributions on the two planes shown in Figs. 5(a) and 5(b), respectively. The false target never generated a meaningful peak. In the optical experiment, the obtained CGH was displayed on the SLM and illuminated by a plane wave as shown in the lower part of Fig. 1, the correlation results were reconstructed from the CGH, and depicted in Fig. 6. Fig. 6(a) recorded at $z_0$=2.6cm shows the correlation peak of the front true target, whereas Fig. 6(b) recorded at $z_0$=-2.5cm depicts the correlation peak of the back true target. The false target still never generated a meaningful correlation peak. The 3-D plots of Fig. 6(a) and 6(b) are depicted in 6(c) and 6(d), respectively. The experimental results are consistent with the simulation results, although the optical reconstruction system induces noise, which is not predicted by the simulation. From the obtained correlation results one can easily detect the two true targets, and locate them as well, in their 3-D space. The correlation strength along $z_0$-axis is also investigated in this experiment. Correlation peaks' intensities along $z_0$-axis, at their maximal transverse points, are shown in Fig. 7.

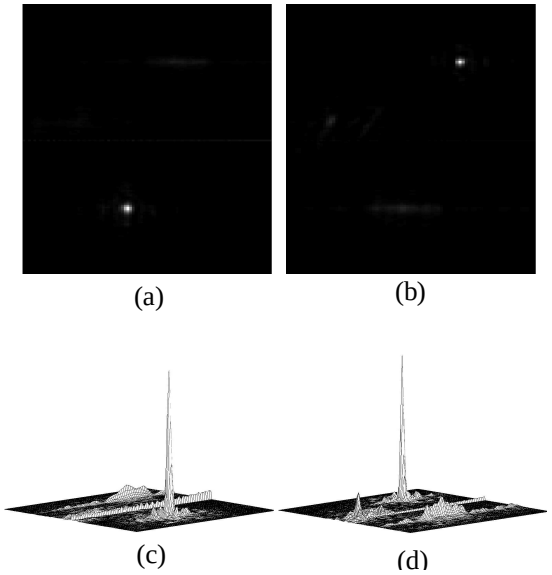


**Fig. 5** The simulated correlation results recorded at (a) $z_0$ = 12.5 pixels (b) $z_0$ = –12 pixels, (c) and (d) are their 3-D plots, respectively.

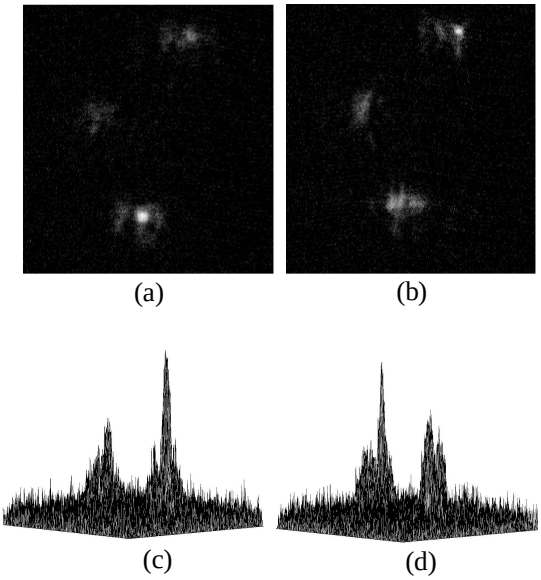


**Fig. 6** The experimental correlation results recorded at (a) 2.6cm and (b)-2.5cm along the $z_0$-axis. Their 3-D plots are shown in (c) and (d), respectively.

The proposed system was compared with the results of the hybrid BGU correlator[6] with two kinds of filters and with two measures. One measure of the performance is signal-to-noise ratio (SNR) indicating the discrimination capability and defined by

$$\text{SNR}=\frac{\text{Maximum correlation peak intensity of the true target}}{\text{Maximum noise intensity}} \qquad (11)$$

Another criteria is peak-to-correlation energy (PCE)[14] indicating the correlation peak sharpness and defined by,

$$\text{PCE} = \frac{\text{Maximum correlation peak intensity of the true target}}{\text{Average correlation plane energy}} \qquad (12)$$

where the average correlation plane energy is defined as the sum of the entire correlation plane intensity divided by the total pixels on a correlation plane. The two criterions are defined on some specific transverse planes, where the peaks of the true objects are maximal. Different filters such as the conventional matched filter and the POF were employed in both 3-D OQC and the hybrid BGU correlator in order to compare their performances. The results of SNR and PCE are calculated accordingly, and summarized in table 1. The SNR and PCE for 3-D OQC are summarized in table 1 column 3 and those for BGU correlators are in column 4. From table 1, one can conclude that although the performances of 3-D OQC are acceptable for different filters, the performances of BGU correlators are superior. This is a reasonable penalty

we should bear due to the use of less information in 3-D OQC than that in the BGU correlators. However, as mentioned above, when the imaging process is carried out along the entire transverse directions, the generated hologram will be $\tilde{T}(u,v)$ rather than $T(u,v)$. Thus the above-mentioned astigmatism will be eliminated, and the performances of 3-D OQC can be improved.

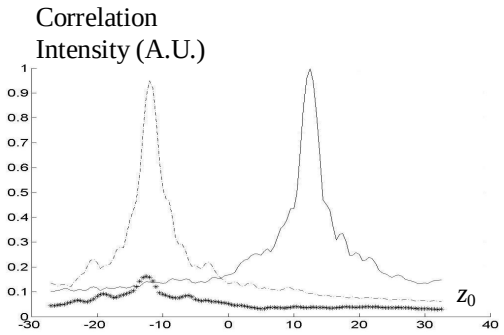


**Fig. 7** The simulated correlation plot along $z_0$-axis. The dash point and line denotes the case of the back true object; the asterisk denotes the false object, and the solid line denotes the front true object.

**Table 1** Summary of the SNR and PCE between the hybrid BGU correlator and the 3-D OQC for two kinds of filters. MF- Matched filter; POF- phase-only filter

| Performance Criteria | Filters | 3-D OQC | BGU Correlators |
|---|---|---|---|
| SNR | MF | 1.8 | 17.8 |
| | POF | 7.3 | 21.6 |
| PCE | MF | 179.6 | 1493.6 |
| | POF | 1499.7 | 3647.1 |

## 4. CONCLUSION

In conclusion, we have proposed a novel method named 3-D OQC to implement 3-D object recognition. By fusing several projections of the tested scene and with proper filtering, a 2-D hologram of the correlation between the tested scene and the reference function is digitally generated. The correlation results are reconstructed when the single hologram is coherently illuminated. The simplicity and speed of the OQC are superior over those of the BGU correlators. However, because of less information used in the 3-D OQC than in the BGU correlators, the method suffers from some penalty of lower SNR and lower PCE in comparison to the BGU correlators. The OQC performances can be improved when symmetrical scanning process is carried out. The method of a single hologram is general and applicable even to circumstances where the objects are occluded from some viewpoints or their shapes are changed as the camera moves. This generality statement is based on our knowledge about holograms of 3-D objects which can image partially occluded objects from certain points of view.

Another unique motive in this study is the nature of the 3-D correlation space. For the best of our knowledge, it is the first time that someone suggests and demonstrates a reconstruction of 3-D correlation space from a single hologram. This innovation should be accompanied by a new concept of detection of the correlation results. One possible option is to let a human observer to look over the correlation space and to estimate the locations of all the true targets in the scene.

## *Reference*


1. R. Bamler, J. Hofer-Alfeis, "Three- and four-dimensional filter operations by coherent optics," Opt. Acta **29**, 747-757 (1982).
2. J. Rosen, "Three-dimensional optical Fourier transform and correlation," Opt. Lett. **22**, 964-966 (1997).
3. J. Rosen, "Three-dimensional electro-optical correlator," J. Opt. Soc. Am. A **15**, 430-436 (1998).
4. J. Rosen, "Three-dimensional joint transform correlator," Appl. Opt. **37**, 7538-7544 (1998).
5. Y. Li, J. Rosen, "Three-dimensional pattern recognition with a single two-dimensional synthetic reference function," Appl. Opt. **39**, 1251-1259 (2000).
6. Y. Li, J. Rosen, "Three-dimensional correlator with general complex filters," Appl. Opt. **39**, 6561-6572 (2000).
7. J. J. Esteve-Taboada, D. Mas and J. Garcia, "Three-dimensional object recognition by Fourier transform profilometry," Appl. Opt. **38**, 4760-4765 (1999).
8. Y. Frauel, E. Tajahuerce, M.-A. Castro, and B. Javidi, "Distortion-tolerant three-dimensional object recognition with digital holography," Appl. Opt. **40**, 3887-3893 (2001).
9. O. Matoba, E. Tajahuerce, and B. Javidi, "Real-time three-dimensional object recognition with multiple perspectives imaging," Appl. Opt. **40**, 3318-3325 (2001).
10. M. Takeda and K. Mutoh, "Fourier transform profilometry for the automatic measurement of 3-D object shapes," Appl. Opt. **22**, 3977-3982 (1983).
11. Y. Li, D. Abookasis, and J. Rosen, "Computer-generated holograms of three-dimensional realistic objects recorded without wave interference," Appl. Opt. **40**, 2864-2870 (2001).
12. J. Rosen, "Computer-generated holograms of images reconstructed on curved surfaces," Appl. Opt. **38,** 6136-6140 (1999).
13. O. Bryngdahl and F. Wyrowski, "Digital holography - computer-generated Holograms," Prog. In Optics, E. Wolf, ed. (North Holland, Amsterdam, 1990) Vol. **28**, pp. 1-86.
14. V. K. Vijaya-Kumar and L. Hassebrook, "Performance measures for correlation filters," Appl. Opt. **29,** 2997-3006 (1990).